

# Elemental abundances in the center of the Galactic Nuclear Disc

V. V. Kovtyukh<sup>1,2\*</sup>, S. M. Andrievsky<sup>1,2,3</sup>, R. P. Martin<sup>4†</sup>, S. A. Korotin<sup>5</sup>,  
J. R. D. Lepine<sup>6</sup>, W. J. Maciel<sup>6</sup>, L. E. Keir<sup>1</sup>, E. A. Panko<sup>7</sup>

<sup>1</sup>*Astronomical Observatory, Odessa National University, Shevchenko Park, 65014 Odessa, Ukraine*

<sup>2</sup>*Isaac Newton Institute of Chile, Odessa Branch, Shevchenko Park, 65014 Odessa, Ukraine*

<sup>3</sup>*GEPI, Observatoire de Paris-Meudon, CNRS, Université Paris Diderot, 92125 Meudon Cedex, France*

<sup>4</sup>*Department of Physics and Astronomy, University of Hawai'i at Hilo, Hilo, HI, 96720, USA*

<sup>5</sup>*Crimean Astrophysical Observatory, Nauchnyy 298409, Republic of Crimea*

<sup>6</sup>*Instituto de Astronomia, Geofísica e Ciências Atmosféricas da Universidade de São Paulo, Cidade Universitária, CEP: 05508-900, São Paulo, SP, Brazil*

<sup>7</sup>*Department of theoretical physics and astronomy, Odessa National University, 42 Pasteur Str., Odessa, Ukraine*

Accepted 2019 August 14. Received 2019 August 1; in original form 2019 April 9

## ABSTRACT

We have made the first attempt to derive the chemical properties of the Galactic disc at its very central part using high-resolution infrared spectroscopic observations of four classical Cepheids. Those stars are located at Galactocentric distances smaller than 1 kpc. All investigated stars show near-to-solar elemental abundances. By combining these new data with our previous studies, this result suggests that the radial distribution of iron abundance on a logarithmic scale gradually increases from the outskirts of the Galactic disc to Galactocentric distances of about 2–4 kpc, reaching there a maximal value of about +0.4 dex, and then declines sharply to about the solar value at the Galactic Center.

**Key words:** stars: abundances – stars: Cepheids – Galaxy: evolution

## 1 INTRODUCTION

In our two previous papers on the chemical properties of the central part in the Galactic thin disc (see Martin et al. 2015; Andrievsky et al. 2016), it has been suggested that there is a plateau in metallicity distribution within approximately 2–4 kpc from the Galactic Center. The maximum metallicity here reaches about  $[\text{Fe}/\text{H}] = +0.4$  dex. This value is attained following the more or less radial monotonic increase of the metallicity from the outer parts of the Galactic disc (16 kpc) to the Galactic Center, with a slope in the global  $[\text{Fe}/\text{H}]$  abundance gradient of about  $-0.055$  dex  $\text{kpc}^{-1}$ .

At the same time, several studies (see compilation in Martin et al. 2015) show that the chemical properties at the very Galactic Center are almost the same as those at the Galactocentric distance of the Sun. Thus, within the range

of 0 to approximately 3 kpc, the metallicity gradient even appears to have a positive slope.

It should be noted, however, that the central part of the Galactic thin disc is poorly sampled (see Figs. from Andrievsky et al. 2016). Additional observations are urgently needed to confirm (or disprove) the existence of the metallicity plateau within the very inner disc (which was suspected, in particular, by Andrievsky et al. 2016) and, also to determine its characteristics (slope, level) if present.

Of particular interest is the determination of the metallicity in the center of the Nuclear Disc. Several studies have been devoted to this topic. In 2000, Carr et al. studied the infrared spectra of M2 IRS, a supergiant which is less than 10 million years old and located near the Galactic Center. They found a solar metallicity for this star (within the measurement errors). Moreover one M supergiant RV 5-7, located at a Galactocentric distance of less than 30 pc, was studied by Ramírez et al. (2000). These authors also found a solar metallicity value for that star. Cunha et al. (2007) also analyzed spectra of several cool supergiants including IRS 7 and VR 5-7. They derived masses of 22 and 14 solar masses for those stars, respectively, indicating relatively young ages.

\* E-mail: vkovtyukh@ukr.net

† Visiting astronomer at the Infrared Telescope Facility, which is operated by the University of Hawaii under contract NNN14CK55B with the National Aeronautics and Space Administration.

The mean  $[\text{Fe}/\text{H}]$  value derived for the sample of M supergiants was  $+0.14$  dex. Similarly, Ryde & Schultheis (2015) determined the metallicity in M giant stars, and found a mean  $[\text{Fe}/\text{H}] = +0.11$  dex.

Summarizing, it can be stated that young M supergiants and older M giants located in the Galaxy Center exhibit solar-like metallicity. It should also be noted that so far, no one has used Cepheid variable stars to determine the metallicity within the young Nuclear Disc.

Some similar results have been pointed out from studies focusing on planetary nebulae in the direction of the Galactic Center (see, for example, Cavichia et al. 2011 and Gutenkunst et al. 2008). According to those programs, the abundances of some elements in the very central part of our Galaxy appear to be close to the solar values. This is an interesting result and it requires an independent verification by obtaining and analyzing the spectra of stars that definitely belong to the Galactic Nuclear Disc.

At present, existing theoretical models focusing on the chemo-dynamical evolution of the Galaxy disc use modern data on the elemental yields in stars of different masses, take into account interstellar gas flows in the disc and halo, as well as the dynamic influence of the Galactic bar on the chemical properties in the Galactic Center, etc. Therefore, elemental distributions in the disc obtained from observations are important criteria for verifying the reliability of those models.

For instance, Minchev et al. (2013) performed a study of the Galaxy thin disc chemical evolution through models. According to their results, the metallicity of  $[\text{Fe}/\text{H}]$  in the disc gradually increases from a Galactocentric distance of 15 kpc to 2 kpc, reaching a plateau in 0 to 2 kpc range, with a maximum value of  $[\text{Fe}/\text{H}]$  of about  $+0.7$  dex (see their Fig. 2). Similarly, Cavichia et al. (2014) obtained a plateau in the radial iron distribution in the range of Galactocentric distances from 0 to 4 kpc. The maximum value  $[\text{Fe}/\text{H}]$  obtained by those authors is  $+0.4$  dex.

Additionally, Kubryk et al. (2015) have developed models including calculations up to a Galactocentric distance 1 kpc. Although their  $[\text{Fe}/\text{H}]$  value at a distance of 3–4 kpc from the Galactic Center is in good agreement with our observational data from Andrievsky et al. 2016 (a small plateau in the iron abundance distribution within this zone with  $[\text{Fe}/\text{H}] \approx +0.4$  dex, see their Fig. 5), their model predicts a steady grows of metallicity toward the Center with  $[\text{Fe}/\text{H}] \approx +0.7$  dex at a Galactocentric distance of 1 kpc.

Recent results presented by Toyouchi & Chiba (2018) show that their model predicts a metallicity  $[\text{Fe}/\text{H}]$  at the level of about  $+0.6$  dex at a Galactocentric distance of 2 kpc (which is close to our observational result, see Andrievsky et al. 2016). Unfortunately those authors did not study the chemical properties of the stellar disc component in the Milky Way Center.

Recently Dékány et al. (2015) and Matsunaga et al. (2015) reported the photometric discovery of several classical Cepheids which are distributed around and behind the Galactic Center. To observe spectroscopically the Galactic Center Cepheids is a very difficult task. Extremely strong light absorption makes it impossible to get high resolution spectra of those stars in the visible. Therefore we decided to observe several targets from the list of Matsunaga et al. (2016) in H spectral band in order to avoid significant light

absorption. It should be also noted that recently Inno et al. (2019) applied IR spectra of medium resolution ( $R = 3000$ ) of five newly discovered Cepheids in the direction of the Galactic Center, but their program stars are situated at a few kpc from the center.

## 2 OBSERVATIONS AND DATA REDUCTION

Near-IR spectroscopic observations were carried out in remote observing mode on two half-nights (May 11 and May 17, 2017), with the InfraRed Telescope Facility (IRTF) 3-meter telescope on Maunakea. We used the recently commissioned cross-dispersed echelle spectrograph iShell (1.08–5.3 micron,  $R = 80000$ , Rayner et al. 2016). The detector was binned  $2 \times 2$  resulting in a spectral resolution  $R \approx 35000$ ; a  $0.75'' \times 5''$  slit was used for all observations. With the H1 instrumental configuration for the spectrograph, the wavelength coverage extended from 1.48 to 1.67  $\mu\text{m}$ , a bandpass including important spectral lines needed for the abundance analysis of our program Cepheids. Observations were conducted under photometric skies, with a seeing of  $0.5'' - 0.8''$  in the visible. For each Cepheid star (typical magnitude  $H \approx 12$ ), exposures were  $6 \times 600$  seconds (coadds). The latter strategy was selected to achieve  $S/N \geq 30$ , a minimum necessary to perform the analysis of the main spectral lines within the H1 bandpass; the exposure times were estimated using the iShell performance established during commissioning of the instrument by IRTF.

A reference solar spectrum ( $4 \times 5$  seconds) was also obtained by observing the Moon. This spectrum is used to verify values for transition oscillator strengths known from literature. A series of spectra was also obtained on several well-studied F and G supergiants.

An observational challenge for our program was to correctly identify the right targets to position them within the spectrograph slit since all inner disc Cepheids are obviously located in very crowded fields. To achieve this, we first applied offsets relative to nearby reference stars instead of only relying on the accuracy of the telescope absolute pointing. These telescope offsets were calculated using the precise coordinates given by Matsunaga et al. (2016) for our four Cepheids. From our experience, this technique brought the targeted Cepheid within a few arcseconds from the spectrograph slit. We then compared the guider field of view with finding charts (see Figure 1) centered of the Cepheid coordinates from Matsunaga et al. (2016) and extracted from K-band images from the 2MASS survey using the Finder Chart tool at [irsa.ipac.caltech.edu/applications/finderchart/](http://irsa.ipac.caltech.edu/applications/finderchart/). All Cepheid stars of our program were clearly visible in the guider; direct comparison with the 2MASS finding charts was possible since we also used a K-band filter in the telescope guider (field-of-view of  $42''$ ). A final (manual) offset was then applied to bring the target Cepheid precisely within the narrow slit of the spectrograph. As shown also in Fig. 1, the iShell slit is only  $5''$  in length and care was taken as well to avoid spectral contamination by other stars within the field, at least from objects we could visually detect within the guider.

For wavelength calibration and for removing the telluric absorption lines, we also observed telluric standard stars (B- and A-type dwarfs). Spectra were combined into a single

spectrum for each target. The telluric absorption lines of the target were subtracted using a spectrum of the corresponding telluric standard.

As an additional check that we indeed observed the same Cepheids as sampled by Matsunaga et al. (2015), we measured the radial velocities of our targets using telluric lines as the wavelength reference frame. The results are shown in Table 1. The velocities obtained were then transformed into barycentric velocities,  $V_{\text{bary}}$ , and velocities relative to the local standard of rest (LSR),  $V_{\text{LSR}}$ , assuming the standard solar motion (Reid et al. 2009, see Table 1). All radial velocities show good fit with the radial velocity curves given in Matsunaga et al. 2015 (see our Fig. 2 and their Fig. 6). Pulsational phases were calculated according to the data of Matsunaga et al. (2015). To control our results, we also determined the radial velocities of the F and G supergiants observed for our program. Our results are in a good agreement with the literature data (see Table 2). Note that HD 182296 is a spectroscopic binary star. Thus, we are confident that our faint targets have been correctly identified.

The details of observations are provided in Table 1.

### 3 SPECTROSCOPIC ANALYSIS

In order to normalize the individual spectra to the local continuum, to identify the lines of different chemical elements, and to measure the equivalent widths (EW) of the absorption lines, we used the DECH 30 software package<sup>1</sup>. Fragments of the spectra of our program Cepheids are shown in Fig. 3.

As we can see from Fig. 3, the spectra are rather noisy, but some lines can be measured with a reasonable precision.

The effective temperatures ( $T_{\text{eff}}$ ) of our program F–G supergiants have been estimated using the calibrating IR line depth ratios, as explained in Fukue et al. (2015). In the Table 2 we give the resulting temperature values determined using IR and visual spectra. The values of  $T_{\text{eff}}$  for visual spectra are based on the use of Kovtyukh (2007) calibrating line depth ratio method. As can be seen, independent estimates are in fairly good agreement.

The effective temperatures of our program Cepheids have also been estimated using the calibrating line depth ratios from Fukue et al. (2015) (see Table 3).

For bright supergiant stars, the surface gravity is estimated from the ionizational balance for iron using the visual spectrum; this value is then adopted for the near-IR spectroscopic analysis (measurable FeII lines are not available in the H-band region). Since we had not enough FeII lines for Cepheids, we were not able to estimate surface gravity using the typical condition of ionization balance. In this case we roughly evaluated  $\log g$  with the help of approximate relation between surface gravity of Cepheids and their pulsational period (see Fig. 5 in Andrievsky et al. 2005).

The microturbulent velocity  $V_t$  for our program stars was found by avoiding any dependence between the iron abundance as produced by individual FeI lines and their equivalent widths.

The resulting atmosphere parameters and other information for the studied stars are listed in Table 3.

Approximated accuracy of our parameter determination is estimated to be:

$$\begin{aligned} \Delta T_{\text{eff}} &= \pm 200 \text{ K}, \Delta \log g = \pm 0.3 \text{ dex}, \\ \Delta V_t &= \pm 0.5 \text{ km s}^{-1}, \Delta [\text{Fe}/\text{H}] = \pm 0.2 \text{ dex}. \end{aligned}$$

### 4 ABUNDANCE ANALYSIS

The local thermodynamical equilibrium elemental abundances in our program stars were calculated using the WIDTH9 code and ATLAS12 atmosphere models. For that purpose, we used newly evaluated astrophysical oscillator strengths and damping parameters adopted by the Apache Point Observatory Galactic Evolution Experiment (APOGEE, Shetrone et al. 2015, their Table 7).

Abundances in two supergiants were derived in order to check the reliability of our H-band spectroscopic analysis. For these stars we compared abundances derived from H-band spectra with abundances derived from the visual spectra. Results for H-band are presented in Table 4 for one star, HD 179784.

Resulting abundances for our program Cepheids are given in Table 5.

### 5 RESULTS AND DISCUSSION

The steady decrease of metallicity with Galactic radius as observed for Cepheids can be interpreted in a simple way. Excluding the possibility of a large radial excursion of the Cepheids, since these stars are very young, their metallicity reflects the local abundance of the interstellar medium (ISM), at their current Galactic radius. The enrichment of the ISM is mostly due to the explosion of supernovae (Matteucci et al. 2009). Since the Initial Mass Function seems to be universal, the formation rate of stars of all masses in just in proportions given by the IMF. A region where the density of stars is large is a region where the star formation rate and the duration of the star forming process were large. Therefore, we expect that the metallicity at a given radius of the disc should be proportional to the stellar density. Thus, it is important to establish what the stellar density is in the thin disc as a function of radius. Many authors consider that the disc density is exponential (Robin et al. 2003) according to a law which extends (or not) up to the center. A disc profile proposed by Kormendy (1997), mostly based on observations of external galaxies, seems close to reality. The law for the surface density is  $\Sigma = \Sigma_0 \exp(-r/\alpha - (\beta/r)^n)$ , where  $\alpha$  is the scale length of the disc and  $\beta$  the "size" of the hole;  $n$  is taken equal to 2. This law produces a decrease of  $\Sigma$  for values of  $r$  smaller than  $\beta$ . The metallicity data is a logarithmic scale, so that we should compare it with  $\log(\Sigma)$ . If we adopt  $\beta$  of the order of 2 kpc, following Lépine & Leroy (2000), this disc profile predicts a maximum metallicity around  $r = 2$  kpc, in satisfactory agreement with our Cepheids' data.

However, the central region of the Galaxy is far from being axi-symmetric, due to the presence of the bar. A recent sketch of the bar, with its extension and orientation in a direction not far from that of the Sun (about  $20^\circ$ ),

<sup>1</sup> <http://www.gazinur.com/DECH-software.html>

**Table 1.** Journal of observations.

Cepheid	N	R.A. J2000.0	Dec J2000.0	Date UTC	JD(start) 2457000+	Phase	Integ. Time s	S/N	$V_{\text{bary}}$ $\text{km s}^{-1}$	$V_{\text{LSR}}$ $\text{km s}^{-1}$	Airmass
GCC-a	13	17:46:06.0	-28:46:55.1	May 18, 2017	892.0150	0.86	$7 \times 600$	30	155.0	165.4	1.52
GCC-b	12	17:45:32.3	-29:02:55.3	May 18, 2017	891.9552	0.29	$6 \times 600$	35	-84.0	-73.7	1.60
GCC-c	11	17:45:30.9	-29:03:10.6	May 12, 2017	886.0177	0.56	$6 \times 600$	33	-70.2	-59.9	1.51
GCC-d	10	17:44:56.9	-29:13:33.8	May 12, 2017	885.9623	0.79	$6 \times 600$	37	-11.9	-1.7	1.61
HD 172594		18:41:42.5	-14 33 51.3	May 12, 2017	886.0595	-	$2 \times 20$	100?	-2.8	11.2	1.21
HD 179784		19:13:15.4	+15 02 08.3	May 18, 2017	892.0755	-	$3 \times 10$	100?	-21.2	-2.6	1.00
HD 182296		19:23:38.7	+08 39 36.0	May 18, 2017	892.0781	-	$4 \times 10$	100	-12.0	5.6	1.02

Remarks: The name of Cepheid is from Matsunaga et al. (2015). The number N is given according to the designation of Matsunaga et al. (2016). Phases were calculated according to the data of Matsunaga et al. (2015).

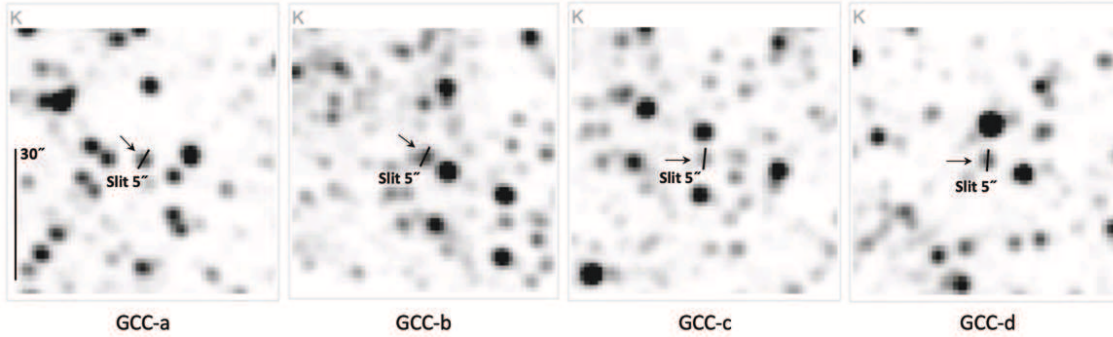


**Figure 1.** Finding charts for the four inner disc Cepheids studied for this program. The field-of-view is  $60'' \times 60''$ , similar to the field available for the iShell spectrograph guider; sky images were extracted from the 2MASS survey in K-band. Each individual field is centered on the coordinates for the Cepheids as published by Matsunaga et al. (2016); each target put within the iShell slit is identified by an arrow. The field scale is displayed in the left image. The slit is by default at the parallactic angle. We took care that for each angle, no other star than our target was seen in the slit. The  $5''$  slit is displayed directly on the target, including the angle of the slit as used during the observation. It is clear that there is no contamination from field stars. North is at the top, east at the left.

**Table 2.** Comparison of the temperature and radial velocity values for supergiants determined from visual and H-band spectra for three supergiants.

HD	Sp	$T_{\text{eff}}(\text{visual})$ (Kovtyukh 2007)			$T_{\text{eff}}(\text{H-band})$ (this paper)			Radial velocity	
		$T_{\text{eff}}$ K	$\sigma_{\text{mean}}$ K	N	$T_{\text{eff}}$ K	$\sigma_{\text{mean}}$ K	N	$V_r$ $\text{km s}^{-1}$	$V_r$ $\text{km s}^{-1}$
172594	F2Ib	-	-	-	-	-	-	-2.8	-2.41
179784	G5Ib	4956	$\pm 42$	55	5054	$\pm 123$	8	-21.2	-21.67
182296	G3Ib	5072	$\pm 50$	77	5059	$\pm 88$	3	-12.0	-9.35...-14.0 SB

Remark: N is a number of used temperature calibrations.  
Typical literature  $V_r$  values can be found e.g. in SIMBAD.

**Table 3.** Physical parameters of the investigated Cepheids.

Cepheid	N	P day	JD, 2457000+ (start)	$\langle H \rangle$ mag	$T_{\text{eff}}$ K	$\log g$	$V_t$ $\text{km s}^{-1}$	$R_G$ kpc
GCC-a	13	23.52	892.0150	12.02	4850	1.0	3.5	$< 0.2$
GCC-b	12	19.96	891.9552	11.96	5050	1.2	3.0	$< 0.2$
GCC-c	11	22.75	886.0177	12.39	5000	1.2	3.0	$< 0.2$
GCC-d	10	18.87	885.9623	12.14	5580	1.4	3.5	$< 0.2$

Remark: The number N is given according to Matsunaga et al. (2016).

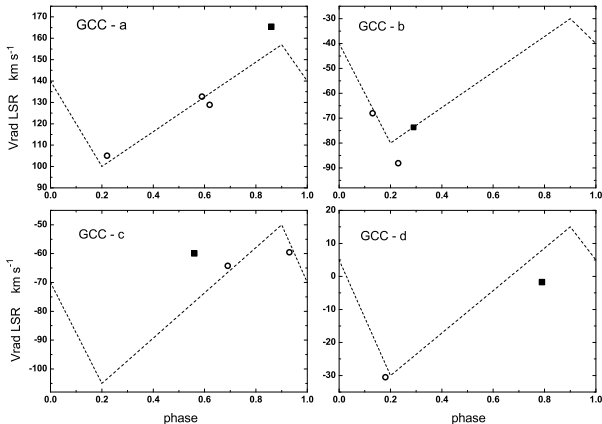


**Figure 2.** Radial velocity curves of the program Cepheids. *Open circles* indicate data from the paper of Matsunaga et al. (2015), *black squares* represent our data. *Dashed lines* schematically show radial velocity curves of Cepheids according to the data from Matsunaga et al. 2015 (see their Fig.6). Deviations of our points from the curve data may be caused by evolutionary changes of periods.

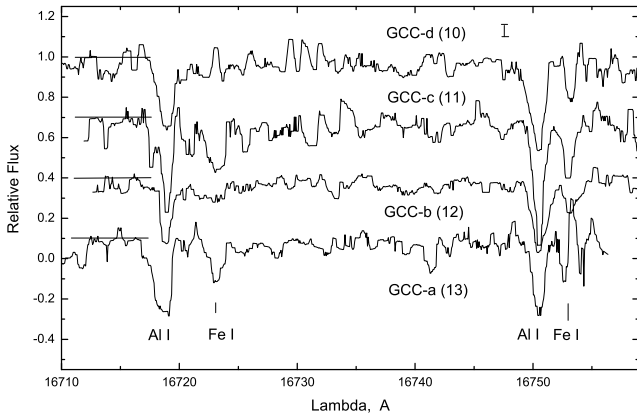


**Figure 3.** Fragments of the spectra of program Cepheids. A portion of the continuum for each spectrum is shown on the left by a *continuous line*.

is presented by Michtchenko et al. (2018) (their Figure 15). In the plane of the Galaxy and for radii  $< 3$  kpc (in the direction of the axis of the bar) the bar dominates the stellar population. There is no star formation in an extended region. The masers with precise VLBI distances measured by Reid et al. (2014), and which are associated with massive stars, are plotted in that figure. The presence of masers signals the regions where very young stars are present. We can see that there are masers all around the bar, but not inside it. Observations of external barred galaxies confirm that most bars are of yellowish color, which indicates that they are mainly constituted of old stellar population. Except maybe for some very late-type, low-mass or weakly interacting barred spirals (see for instance Martin & Friedli 1997), there are no O–B stars in the bar, except at their extremities and at their very center. This also explains the absence of numerous Cepheids in the Galactic radius range 1–3 kpc.

**Table 4.** Comparison of abundances in HD 179784 derived from visual and H-band spectra. Stellar atmosphere parameters are presented in the form  $T_{\text{eff}}/\log g/Vt$

Ion	HD179784 (Visual) 4956/1.8/2.3			HD179784 (H-band) 5054/1.8/2.2		
	[M/H]	$\sigma$	N	[M/H]	$\sigma$	N
6.00	-0.18	0.24	3	-0.40	0.18	6
7.00	–	–	–	0.37	–	1
8.00	0.16	–	1	–	–	–
11.00	0.40	0.02	2	0.38	0.16	2
12.00	-0.11	–	1	0.21	0.04	2
13.00	0.18	0.13	2	–	–	–
14.00	0.07	0.08	10	-0.03	0.14	13
15.00	–	–	–	0.36	0.19	3
16.00	0.35	–	1	0.04	0.12	8
20.00	0.02	0.08	3	0.24	0.07	3
21.01	0.05	0.11	5	–	–	–
22.00	-0.21	0.13	14	0.12	0.10	6
22.01	-0.16	0.13	3	–	–	–
23.00	-0.13	0.12	7	0.02	0.53	5
23.01	0.10	0.13	4	–	–	–
24.00	-0.17	0.10	11	0.02	0.02	3
24.01	0.22	0.10	3	–	–	–
25.00	0.10	0.11	5	-0.04	0.40	6
26.00	0.00	0.10	82	0.12	0.15	156
26.01	0.02	0.12	14	–	–	–
27.00	-0.03	0.14	8	0.16	0.46	6
28.00	-0.03	0.10	36	0.04	0.13	8
29.00	-0.41	0.00	1	-0.11	0.33	2
39.01	0.22	0.07	4	0.36	–	1
40.01	-0.03	0.02	2	–	–	–
57.01	0.17	–	1	–	–	–
58.01	0.01	0.04	4	–	–	–
59.01	-0.06	0.05	2	–	–	–
60.01	0.12	0.07	5	–	–	–
63.01	0.21	0.01	2	–	–	–
64.01	0.38	–	1	–	–	–

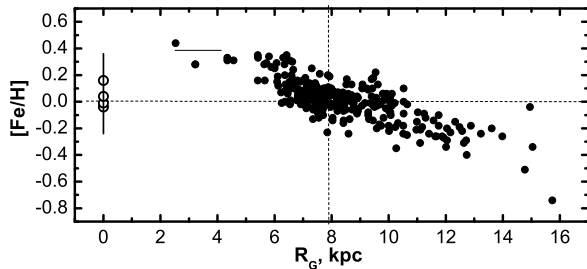


**Figure 4.**  $[\text{Fe}/\text{H}]$  vs  $R_G$ . *Filled circles* – compilation of iron abundance determinations in Galactic Cepheids from our papers published from 2002 to 2016 (see Martin et al. 2015; Andrievsky et al. 2016, for references). The iron abundance in the Galactic Nuclear Center Cepheids is from this paper (the  $[\text{Fe}/\text{H}]$  values are indicated by the *open circle* symbols with error bars). *Two points* at approximately 2 and 3 kpc correspond to ASAS181024-2049.6 and SU Sct positions, respectively. Approximate position of a plateau-like region (if it really exists) is schematically shown by a *thin continuous line*. The position of the Sun is at the intersection of the *dashed lines*.

**Table 5.** Abundances of individual elements for Galactic Center Cepheids.

Ion	GCC-a (13)			GCC-b (12)			GCC-c (11)			GCC-d (10)		
	[M/H]	$\sigma$	N	[M/H]	$\sigma$	N	[M/H]	$\sigma$	N	[M/H]	$\sigma$	N
6.00	-0.21	0.21	4	-0.30	0.16	5	-0.40	0.22	3	-0.25	0.11	5
11.00	0.61	0.09	2	0.46	0.09	2	0.84	-	1	0.62	0.04	2
12.00	0.38	0.17	2	-0.09	0.30	2	0.11	-	1	0.03	0.05	2
14.00	0.04	0.18	8	0.01	0.21	13	0.41	0.28	5	-0.14	0.03	3
16.00	-0.19	0.22	2	-0.44	0.10	6	-0.05	0.20	6	0.09	0.12	6
20.00	-0.02	0.30	2	-0.36	0.18	3	-	-	-	-0.07	0.43	3
22.00	0.37	0.33	4	-	-	-	0.01	0.39	2	0.27	0.11	2
23.00	-0.42	-	1	-0.04	-	1	-	-	-	0.39	0.25	2
24.00	0.27	0.36	2	-0.23	0.11	3	0.44	-	1	-	-	-
26.00	-0.04	0.13	57	-0.01	0.22	106	0.16	0.21	49	0.04	0.18	122
27.00	-0.24	0.10	2	-	-	-	0.38	-	1	-0.08	0.03	2
28.00	0.13	0.22	8	0.13	0.20	7	-0.05	0.13	2	0.18	0.33	4
39.01	-	-	-	0.11	-	1	-0.48	-	1	-0.01	-	1

The region very close to the center ( $R_G < 1$  kpc) is quite different from its surroundings. It contains at least one maser with distance determined by VLBI measurements, at least 4 Cepheids (the ones studied in this work) and a major molecular cloud, Sagittarius B2. The physical conditions in this area are possibly different from those prevailing in the Solar neighborhood. There is possibly an inflow of matter with a high metallicity coming from internal regions to the disc, flowing across the bar, and possibly an inflow of low metallicity gas from the spheroidal bulge. It is beyond the scope of the present work to develop a specific chemical evolution model for the Galactic Center.

In Fig. 4 we show the iron abundance distribution from the Galactic Cepheids based on our previous studies (see references in Martin et al. 2015 and Andrievsky et al. 2016) and the central value obtained in the present study. We were especially interested in the iron content, since this element has the largest number of lines in the spectra studied, and its content was found with a sufficiently high accuracy. We also have the largest statistics on abundance distribution in the disc for iron. In our previous papers we reported on the elemental distribution in the range of Galactocentric distances extending from about 2 kpc to 16 kpc.

The Cepheids of our present program cover a similar pulsation period range as the stars included in our previous samples; thus they share a similar age range. Following the period-age relation for classical Cepheids as proposed by Bono et al. (2005), the age range of the Cepheids in our sample is roughly 20–70 Myr. So, these are young stars, and they should be situated very near their birthplaces.

The average iron abundance at the Galactic Center from literature is presented in Martin et al. (2015) and Andrievsky et al. (2016). That value was mostly determined from the stars covering a larger age range (some of them are members of the Arches/Quintuplet clusters with age of about  $\approx 3$ –9 Myr, while there are the field stars with age of  $\approx 1$  Gyr. Our data on four young classical Cepheids apparently suggest that the metallicity at the very center of our Galaxy disc is approximately solar. This is the main result of this paper. Looking at Fig. 4 one can note that the metallicity gradually increases from the outer part of the thin disc reaching the maximum value of about +0.4 dex at Galac-

tocentric distance in the range from 2 to 4 kpc, and then decreases to about the solar value in the Galaxy Center. In the range 2–4 kpc, we yet cannot confirm or disprove some kind of the plateau-like structure in the metallicity distribution as it was first supposed in Andrievsky et al. (2016), even with our additional data. More observations will be needed. Independent arguments supporting our result can be found in a recent paper by Bovy et al. (2019), which analyzed the APOGEE observational data. These authors clearly found a zone of increased metallicity at a Galactocentric distance of about 4 kpc, while the metallicity at the Center was similar to that measured at the solar Galactocentric distance (see their Fig. 4).

How reliable is our conclusion regarding the maximum abundance at 2–4 kpc? The answer significantly depends on the position of two stars, namely SU Sct and ASAS 181024-2049.6, which were previously analyzed in Martin et al. (2015) and Andrievsky et al. (2016). In those papers we proceeded from the assumption that both are classical Cepheids. Jayasinghe et al. (2018) performed the All-Sky Automated Survey for Supernovae and, as a by-product, they discovered a large number of new variable stars. In particular they found that SU Sct could be a W Vir star, i.e. Cepheid of type II. If this classification is correct, then the distance used in our previous program may be wrong. Nevertheless, it should be noted that the above authors carried out an automatic classification of a large sample of stars without a careful investigation of the individual objects. Therefore, it cannot be excluded that in the case of SU Sct the classification presented may be erroneous. Moreover, type II Cepheids are known to show a strong emission in  $H\alpha$  near maximum, whereas classical Cepheids, as a rule, do not show it. The star of our program SU Sct does not show emission in  $H\alpha$  (we have five spectra of this Cepheid in our disposal, see fragments of those spectra in Fig.5). In addition, type II Cepheids have a metallicity below zero, while SU Sct shows a metallicity of about +0.3 dex. So it is highly probable that SU Sct is a classic Cepheid. ASAS 181024-2049.6 (three spectra obtained in different phases) also does not show any  $H\alpha$  emission, and it also likely a classic Cepheid. Moreover, both these stars are situated very

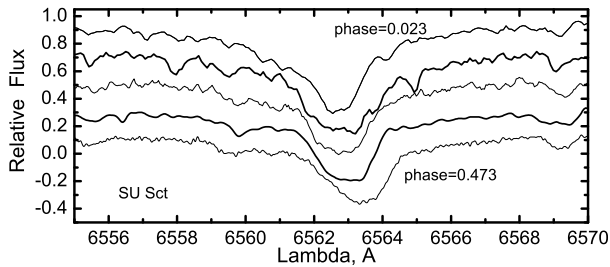


**Figure 5.** Variation of the  $H\alpha$  profile in SU Sct spectra with the pulsation phase. None of the spectra (including the spectrum that was observed at the maximum light) shows any emission feature in this line. Three spectra were collected by Prof. George Wallerstein using the facilities of Apache Point Telescope (priv. comm.) and, the other two were investigated by Martin et al. (2015).

close to the Galactic disc ( $b$  is about  $-6^\circ$  and  $-1^\circ$  respectively), which is not typical for type II Cepheids.

## 6 CONCLUSION

For the first time we derived elemental abundance in fairly young disc stars – Cepheids, which are located in the very center of our Galaxy. We used high-resolution near-IR spectra of four stars observed with the iShell spectrograph attached to the NASA InfraRed Telescope Facility. Our LTE analysis showed that these Cepheids have metallicities close to solar values, a new result for the very central part of the Galactic Nuclear Disc.

## 7 ACKNOWLEDGMENTS

We acknowledge the excellent support team at NASA IRTF and for the iShell echelle spectrograph. The authors wish to recognize and acknowledge the very significant role that the summit of Maunakea has always had within the indigenous Hawaiian community. We are most grateful to have had the opportunity to conduct observations from this mountain over the years. WJM thanks CNPq (Process 302556/2015-0) and FAPESP (Process 2010/18835-3 and 2018/04562-7). Authors are also thankful to the anonymous referee for his/her valuable comments which have considerably improved our paper.

## REFERENCES

Andrievsky S. M., Luck R. E., Kovtyukh V. V., 2005, *AJ*, 130, 1880  
 Andrievsky S. M., Martin R. P., Kovtyukh V. V., Korotin S. A., Lépine J. R. D., 2016, *MNRAS*, 461, 4256  
 Bono G., Marconi M., Cassisi S., Caputo F., Gieren W., Pietrzynski G., 2005, *ApJ*, 621, 966  
 Bovy J., Leung H. W., Hunt J. A. S., Mackereth J. T., Garcia-Hernandez D. A., Roman-Lopes A., 2019, preprint (arXiv: astro-ph/190511404B)  
 Carr J.S., Sellgren K., Balachandran S.C., 2000, *ApJ*, 530, 307

Castelli F., Kurucz R.L., 2004, preprint (arXiv:astro-ph/0405087)  
 Cavichia O., Costa R. D. D., Maciel W. J., 2011, *Rev. Mex. Astron. Astrof.*, 47, 49  
 Cavichia O., Mollá M., Costa R.D.D., Maciel W.J., 2014, *MNRAS*, 437, 3688  
 Cunha K., Sellgren K., Smith V. V., Ramirez S. V., Blum R. D., Terndrup D. M., 2007, *ApJ*, 669, 1011  
 De Medeiros J.R., Udry S., Burki G., and Mayor M., 2002, *A&A*, 395, 97  
 Dékány I., Minniti D., Majaess D., Zoccali M., Hajdu G., Alonso-García J., Catelan M., Gieren W., Borissova J., 2015, *ApJ*, 812, 29  
 Fukue K., Matsunaga N., Yamamoto R., et al., 2015, *ApJ*, 812, 64  
 Gutenkunst S., Bernard-Salas J., Pottasch S. R., Sloan G. C., Houck, J. R. 2008, *ApJ*, 680, 1206  
 Inno L., Urbaneja M.A., Matsunaga N. et al., 2019, *MNRAS*, 482, 83  
 Jayasinghe T., Kochanek C. S., Stanek K. Z. et al. 2018, *MNRAS*, 477, 3145  
 Kormendy J. 1977, *ApJ*, 217, 406  
 Kovtyukh V. V., 2007, *MNRAS*, 378, 617  
 Kubryk M., Prantzos N., Athanassoula E., 2015, *A&A*, 580A, 127  
 Lépine J. R. D., Leroy P., 2000, *MNRAS*, 313, 263  
 Luck R. E., Andrievsky S. M., Kovtyukh V. V., Gieren W., Graczyk D., 2011, *AJ*, 142, 51  
 Martin R. P., Andrievsky S. M., Kovtyukh V. V., Korotin S. A., Yegorova I. A., Saviane I., 2015, *MNRAS*, 449, 4071  
 Martin P., Friedli D., 1997, *A&A*, 326, 449  
 Matsunaga N., et al. 2013, *MNRAS*, 429, 385  
 Matsunaga N., et al., 2016, *MNRAS*, 462, 414  
 Matsunaga N., et al., 2015, *ApJ* 799, 46  
 Matteucci F., Spitoni E., Recchi S, Valiante R., 2009, *A&A*, 501, A122  
 Michtchenko T. A., Lépine J. R. D., Barros D. A., Vieira R. S. S., 2018, *A&A*, 615, 10  
 Minchev I., Chiappini C., & Martig M., 2013, *A&A*, 558, 9  
 Ramírez S.V., Sellgren K., Carr J. S., Balachandran S.C., Blum R., Terndrup D. M., Steed, A., 2000, *ApJ*, 537, 205  
 Rayner J.T., et al., 2016, *SPIE*, 9908E, 84  
 Reid M. J., et al., 2009, *ApJ*, 700, 137  
 Reid M. J., et al., 2014, *ApJ*, 783, 130  
 Robin A. C., Reylé C., Derrière S., Picaud S., 2003, *A&A*, 409, 523  
 Ryde N., Schultheis M., 2015, *A&A*, 573A, 14  
 Shetrone M., Bizyaev D., Lawler J.E. et al., 2015, *ApJS*, 221, 24  
 Toyouchi D., Chiba M., 2018, *ApJ*, 855, 104

This paper has been typeset from a  $\text{\TeX}/\text{\LaTeX}$  file prepared by the author.